J. Chil. Chem. Soc., 69, N°3 (2024)

HYBRID MATERIALS BASED IN METAL-ORGANIC-FRAMEWORKS SUPPORTED ACTIVATED CARBON AS A NOVEL MATERIALS FOR CO2 ADSORPTION FOR ENVIRONMENTAL AND ENERGY APPLICATIONS

PAOLA MÉNDEZ-HERRERA [a,b], ERWIN SEPÚLVEDA SANDOVAL [c,e]*, MARGARITA SEPÚLVEDA REYES [b], RAMÓN AHUMADA RUDOLPH [A], AND VANESSA NOVOA [d]*

[a]*Laboratorio de Química Aplicada y Sustentable, Universidad del Bío-Bío, Av. Collao 1202, Concepción, Chile.*
[b]*Instituto de Transferencia Tecnológica, Concepción, Chile.*
[c]*Centro de Energía, Universidad de Chile, Plaza Ercilla 847, Santiago, Chile.*
[d]*Instituto de Alta Investigación, Universidad de Tarapacá, 18 de septiembre 2222, Arica, Chile.*
[e]*Fraunhofer Chile Research, Bernarda Morin 510, Providencia, Santiago, Región Metropolitana.*

ABSTRACT

A composite of Ni-MOF-5 ($Ni_xZn_{4-x}O(HCOO)_3(BCD)_3$ (0<x<4)) and activated carbon were synthesized through a microwave synthesis method with reflux. Various characterization techniques were performed, including XRD, TGA, SEM, EDS, FT-IR, and BET isotherm. The surface study of the material shows the presence of crystals with a cubic structure of Ni-MOF-5 with sizes smaller than 10 µm. A superficial area of 718 m^2/g and thermostability with a mass loss of 4.72% at 459°C of the metal-organic framework were observed. The results for different CO_2 concentrations at 1 bar and 25 °C show that the adsorption capacity had a linear relationship between % CO_2 and the amount of CO_2 adsorbed by the hybrid material. The results also showed that by increasing the working temperature in the CO_2 adsorption process and keeping the percentage of CO_2 constant, the amount of adsorbed CO_2 decreases linearly. The adsorption kinetics of CO_2 on the prepared hybrid material are consistent with the intraparticle diffusion model, where diffusion is the rate-limiting step. The adsorption of CO_2 is energetically and kinetically favorable due to the micro-mesoporosity of the material that allows the entry of CO_2 molecules into the pores.

Keywords: *Metal-Organic Framework, Activated carbon, Capture, Carbon dioxide*.

1. INTRODUCTION

The high industrial and energy activity of recent decades has increased the generation rate of CO_2 and other greenhouse gases, which has a direct impact on global warming. The concentration of CO_2 in the atmosphere in the middle of 2022 surpassed 50% of the level recorded at the beginning of the industrial revolution in 1750, which was 280 ppm [1]. Today, there are several technological alternatives focused on reducing these emissions, based on renewable energy and political regulations to face the rise of this gas. Carbon Capture and Storage (CCS) has become a well-discussed alternative to capture and reuse the CO_2 emissions [2]. Direct air capture (DAC) of greenhouse gases will play a crucial role in meeting climate change goals, with large-scale implementation. However, despite this consensus, the performance and impact of direct capture have not been sufficiently investigated, resulting in an obstacle to its large-scale implementation in climate change mitigation initiatives. DAC is considered the most attractive option to achieve net negative CO_2 emissions. Nevertheless, other processes such as filtration, absorption, adsorption systems, and others are needed to reach highly pure CO_2 [3].

Therefore, the development and synthesis of new adsorbents that help solve these problems is an important way to accelerate these processes. In this sense, these three-dimensional porous materials formed by a metallic center and an organic ligand (MOFs) appear as a potential alternative to capture CO_2 from different sources. Furthermore, the presence of open metal sites with appropriate geometry and pore size in these materials is directly associated with high adsorption capacity and selectivity [4][5]. One of the main characteristics of MOFs to be used in CO_2 capture is their hydro-stability. Given the ubiquity of water vapor in the real world, the stability of water is the first obstacle to overcome in practical applications of MOFs. To prepare water-stable MOFs, several important strategies have been proposed, such as increasing the bonding strength of building units and introducing hydrophobic units. Many hydro-stable MOFs have been prepared to capture carbon dioxide in various scenarios, including gas decarbonization combustion, direct air capture, and purified raw natural gas [6]. Metal-organic framework materials have certain advantages over other porous materials, such as zeolites and activated carbons, because they have greater flexibility in terms of the design of their structure and control of the size and functionality of their pores. Thus, MOFs with a great diversity of structures and pore sizes have been synthesized [7]. These characteristics make them interesting for selecting the appropriate MOFs in order to avoid diffusion problems and/or favor selectivity.

Additionally, the adsorption efficiency depends on the properties of the metal-organic frameworks, given by the properties of the chemical reagents used and, very important, on the final contact surface. Efficient adsorption-based CO_2 capture requires solid adsorbents with a high adsorption capacity and high selectivity to preferentially capture CO_2 over other gases [8][9]. The value of the specific surface area of the adsorbent materials is very important, since it is associated with the amount of adsorbate that is adsorbed and the physical characteristics of the solid that allow interaction with the gas [10][11][12].

MOF-5 is one of the most studied MOFs of these porous materials. It consists of four $[Zn_4O]^{6+}$ groups in octahedral subunits that are connected to each other by benzene-1,4-dicarboxylate (BDC) groups, to form a porous cubic structure. This structure provides a large specific surface area, an exceptional pore volume, and relatively thermal stability [13]. MOF-5 is poorly hydrostable, because the relatively weak coordination between metal and oxygen allows the attack of water molecules, resulting in a phase transformation and a collapse of the structure [14].

The incorporation of nickel into the structure of MOF-5 affects the structural properties in several ways. The Ni ions substitute the Zn ions in the MOF matrix, which affects the structural integrity and properties of the framework. The shift in vibration frequencies in FTIR spectra indicates that Ni^{2+} substitution occurs at the Zn^{2+} sites. It modifies the crystallinity of the MOFs, decreasing with increasing Ni doping, which is evident in the X-ray diffraction (XRD) patterns. The size of the crystals also varies with the concentration of Ni that is incorporated. In the case of pure MOF-5, the crystal size is approximately 45 nm, which increases to approximately 51 nm in the case of Ni-MOF-5 (1:9) and decreases to 41 nm in the case of Ni -MOF-5 (1:1). One of the most interesting aspects of the incorporation of Ni is that it improves the hydro-stability of MOF-5. The prepared samples were tested for stability against moisture, and it was found that the crystallinity remained intact even after exposure to moisture, indicating improved stability due to incorporation. Research has shown that MOF-5 incorporating Ni not only exhibits larger Langmuir specific surface areas and larger pores than pure MOF-5 but also significantly improves the water resistance of the structure [15][16][17].

Another way to improve hydro-stability is by designing hybrids with carbonaceous materials, which, due to their hydrophobic chemical nature, help to enhance the synthesized hybrid material for its applications in the selective capture of carbon dioxide. Taking into account the advantages and disadvantages of the different materials used in CO_2 adsorption, current research seeks to establish a synergy between these materials, creating hybrid materials where each one provides its benefits, thus reducing the deficiencies of each one separately. Today, different commercial CO_2 capture and/or storage systems are known, using filter systems, mainly in post-combustion CO_2 capture processes and even capturing CO_2 directly from the air [18][19][20]. Cost-effective CO_2 adsorbents are gaining increasing attention as viable solutions to mitigate climate

**Corresponding author email: pamendez@ubiobio.cl, erwin.sepulveda@centroenergia.cl*

change. Studies have synthesized compounds between biochar and CuBTC (B 1:1) that demonstrated a greater CO_2 adsorption capacity under controlled laboratory conditions against industrial conditions (9.8 mmol/g vs6.2 mmol/g, respectively, at 298 K, 1 bar). Furthermore, the composite exhibited remarkable CO_2/N_2 selectivity and improved stability under humid conditions. The enhanced performance can be attributed to the optimization of the number of active sites, porosity, and conservation of all physical and chemical properties of the surface of both original materials [21]. These favorable characteristics make hybridations of composites of carbonaceous materials with metal-organic frameworks promising candidates for industrial applications.

The adsorption of CO_2 on hybrids of porous carbonaceous materials is an attractive alternative because the process is clean and reversible, with lower energy requirements due to the lower adsorption energy compared to other alternatives such as absorption [22]. The greater porosity, specific surface area, and hydrophobicity of the synthesized hybrid materials make these materials much more attractive for CO_2 adsorption processes both at atmospheric pressure and at high pressures, conditions that occur in some industrial processes, such as wine fermentation (agro-industrial applications) and combustion of power plants.

In this study, a hybrid material based on metal-organic frameworks supported on activated carbon was synthesized and characterized. The material was characterized and evaluated for the adsorption of CO_2 at different pressures with a future agro-industrial application.

2. MATERIALS AND METHODS

Microwave Synthesis of hybrid material based in metal-organic framework supported on activated carbon

The pure Ni-MOF-5 (Zn:Ni; 1:10) and Ni-MOF-5 were synthesized through a microwave synthesis method with reflux for 1 hour as follows: 60 g of granular activated carbon (AC) particle size about 2-3 mm (coconut shell) were mixed and modified with HNO_3 (p.a. from Sigma Aldrich), 0.471 g of $Ni(NO_3)_2x6(H_2O)$ (99% from Sigma Aldrich), 4,842 g of $Zn(NO_3)_2x6(H_2O)$ (99% from Sigma Aldrich), and 0.9 g of 1,4-benzene dicarboxylic (H2BCD) (>99% from Sigma Aldrich). The named precursors were dissolved in 150.00 mL of N,N-dimethylformamide (DMF, 99% Winkler), placed in a 1 L glass reactor. The synthesized material was cooled to room temperature and washed with 150.0 mL of N,N-dimethylformamide. Once washed, the product was activated by solvent exchange with acetone (99% Winkler) and dried at 60 °C in an oven with air convection (Biobase model BOV-T70C) and stored in a desiccator with a vacuum valve (Winkler).

Characterization of hybrid material based in metal-organic framework supported on activated carbon

The crystal structure of the MOFs obtained was analyzed in D8 Endeavor X-ray diffractometer equipment, Bruker, USA, with Cu-Kα radiation in a diffractometer. Diffractograms were taken in continuous mode with a scanning speed of 10°/min, a step of 0.02° in 2θ. To study the chemical structure and the main functional groups present in the synthesized materials, the Perkin Elmer Spectrum BX FT-IR System (Waltham, MA, USA) was used. To carry out the analysis, a potassium bromide tablet and samples were prepared in the study in a 1:100 ratio. The homogenized mixture was subjected to 3000 lbs. of pressure to form the tablet that is measured in the equipment. The surface morphology and particle size of pure Ni-MOF-5 and Ni-MOF-5-AC, as well as their distribution in activated carbon, were evaluated by scanning electron microscopy (SEM) using a JEOL JSM, 6380 V (JEOL, Ltd, Tokyo, Japan). The thermal stability of the materials at different temperatures was made by means of thermal gravimetric analysis (TGA). Pure Ni-MOF-5 and Ni-MOF-5-AC samples were carried out into a Precisa XM60 analyzer for a temperature range from 25 °C to 600 °C and a heating rate of 10 °C/min. using titanium capsules. The BET surface area was obtained with an ASAP2020M analyzer (Micromeritics, USA) with the N2 adsorption–desorption isotherms measured at 77 K, and the samples were pretreated at 423 K under vacuum for 6 h before analysis.

CO_2 adsorption performance

The material was sieved to a granulometry between 106 and 380 µm and placed in a 3/8” stainless steel tube supported by quartz wool. The tube is located inside a temperature-controlled oven; the gases under study are introduced, and subsequently, the gases leaving the reactor are analyzed online with a mass spectrometer. To purge the system, N_2 was used with a flow rate of 50 ml min^{-1} for at least 60 minutes until a steady state was confirmed in the mass spectrometer signal. The temperature was adjusted by heating at 5°C min^{-1} from room temperature to the adsorption temperature. The kinetics of CO_2 adsorption were also studied. The amount of CO_2 adsorbed is calculated by the integration difference of the CO_2 concentration curves as a function of time between the blank experiment (reactor without sample) and the adsorption experiment with the sample. Different CO_2 adsorption experiments were carried out (Table 1). In the experiments, the change in concentration of all the components of the gas mixture used was recorded using the mass spectrometer. (m/z 44 for CO_2, m/z 40 for Ar, and m/z 28 for N_2). Note that the experiments 2, 4 and 5 were made for 15% CO_2 in the input stream, varying the adsorption temperature, while the experiments 1,2, and 3 were made at 25°C, varying the input concentration. The reproducibility of the methodology was evaluated by comparing the results with MgO as a reference material for CO_2 adsorption. The experiments were carried out at room temperature and atmospheric pressure (25 °C, 1 atm).

3. RESULTS

Structural and morphological characterizations

Characterization of hybrid material based in metal-organic framework supported on activated carbon

Pure Ni-MOF-5 and Ni-MOF-5-AC samples were prepared by the microwave synthesis method in a short time of 60 min. Scanning electron microscopy (SEM) and X-ray diffraction (XRD) were applied to characterize the morphology and crystallinity of the samples. Figure 1a shows that Ni-MOF-5 crystals were successfully deposited on the surface of the activated carbon. A large number of Ni-MOF-5 crystals with well-defined cubic structure and different sizes are shown on the external surface and in the pores of the activated carbon. The porous structure of the activated carbon is maintained, and a large amount of the metal organic frameworks have been linked to the surface of the activated carbon both inside and outside the pores. A size distribution analysis of the crystals (Figure 1b) was performed, which allowed us to identify how the Ni-MOF-5 crystals are distributed on the activated carbon surface. The results indicate that the distribution has a log-normal tendency, which is common in nanostructured materials [23], i.e., most of the particles are grouped around an average size with a gradual distribution. An average value of Ni-MOF-5 of 3.55±0.22 µm was obtained, with a range between 0.13 and 12.54 µm. It was also observed that 90% of the crystals were below 6.5 µm, indicating a high concentration of small crystals, which means an advantage for adsorption applications [24].

a)

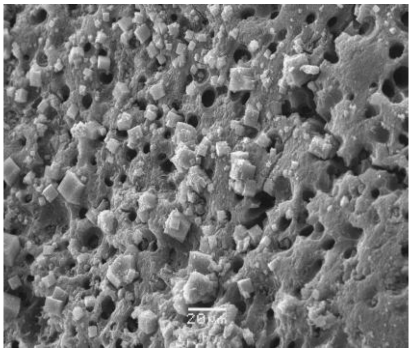

b)

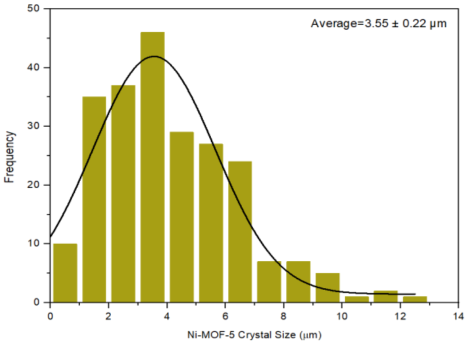

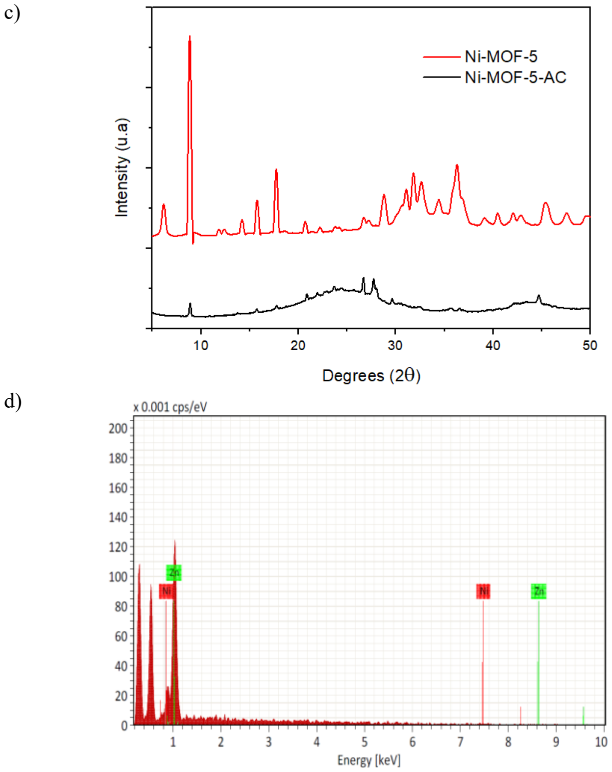

Figure 1. ***a)*** *SEM Ni-MOF-5-AC* ***b)*** *particle size distribution* ***c)*** *DRX* ***d)*** *EDS*

Figure 1c shows the XRD pattern of the pure Ni-MOF-5 and Ni-MOF-5-AC samples. The pure Ni-MOF-5 phase exhibits sharp peaks indicating a well-defined crystallinity. The Ni(II) ions should be well incorporated into the MOF-5 structure, partially replacing the Zn(II) ions from the present $[Zn_4O]^{6+}$ clusters, which is evidenced by energy dispersive X-ray spectroscopy (EDS) (Figure 1d).

Four main diffraction peaks (6.2°, 8.9°, 14.2°, and 15.8°) are observed, very close to those reported for the Ni-MOF-5 crystalline structure. Another main peak appears at 17.7° in the XRD pattern of Ni-MOF-5, probably due to the incorporation of Ni^{+2} in the crystalline structure. The presence of smaller, sharp peaks (31.8°, 34.4°, and 36.3°) was also observed, which according to references is due to the fact that the Ni-MOF-5 structure trapped a trace amount of ZnO [25]. Additionally, Figure 1(c) shows the amorphous phase of activated carbon and the clear presence of the 8.9°, 15.8°, 26.7°, 28.7°, and 44.7° peaks of Ni-MOF-5 in its structure, indicating that Ni-MOF-5 has been incorporated into the activated carbon structure, forming a hybrid material.

The FTIR spectrum is shown in Figure 2a. Here, the adsorption bands corresponding to the vibrations of the functional groups present in the structure of pure Ni-MOF-5 and Ni-MOF-5-AC can be identified. The bands around 1600-1400 cm^{-1} are associated with the stretching vibrations of C=O and C=C bonds. It is confirmed that the carboxylate groups are coordinated with zinc and nickel. The peaks at 1596 cm^{-1}, 1388 cm^{-1} of pure Ni-MOF-5 and 1628, 1388 cm^{-1} of Ni-MOF-5-AC are related to the asymmetric and symmetric stretching vibrations of COO^- group, respectively. The bands in the region between 400 - 600 cm^{-1} present in pure Ni-MOF-5 generally occur due to metal-oxygen stretching vibrations, which is crucial to understanding the coordination that occurs between metals in the MOF structure. These bands are not observed so clearly in the spectrum of Ni-MOF-5-AC, because the MOF is present in approximately 15% of the total mass of the hybrid compound. In both spectra, broad bands near 3400 cm^{-1} are observed, corresponding to the vibration of the O-H group, associated with hydroxyl groups or water adsorbed by the MOF; in the case of Ni-MOF-5-AC, they are also due to oxygenated groups present in the activated carbon. In both pure Ni-MOF-5 and Ni-MOF-5-AC, bands associated with C-H vibrations are observed in the range of 2800 to 3000 cm^{-1}.

The textural properties of the synthesized Ni-MOF-5-AC were determined by nitrogen adsorption test to analyze the specific surface area and pore volume. A typical type I adsorption isotherm behavior was recorded with significant gas uptake at low relative pressure ($P/P^0 < 0.01$), which was followed by a long horizontal plateau extending up to high relative pressure, indicating a typical microporous structure. The specific surface area of the prepared Ni-MOF-5-AC was 718 $m^2\ g^{-1}$, and the pore size was 0.355 $cm^3\ g^{-1}$ (Figure 2b).

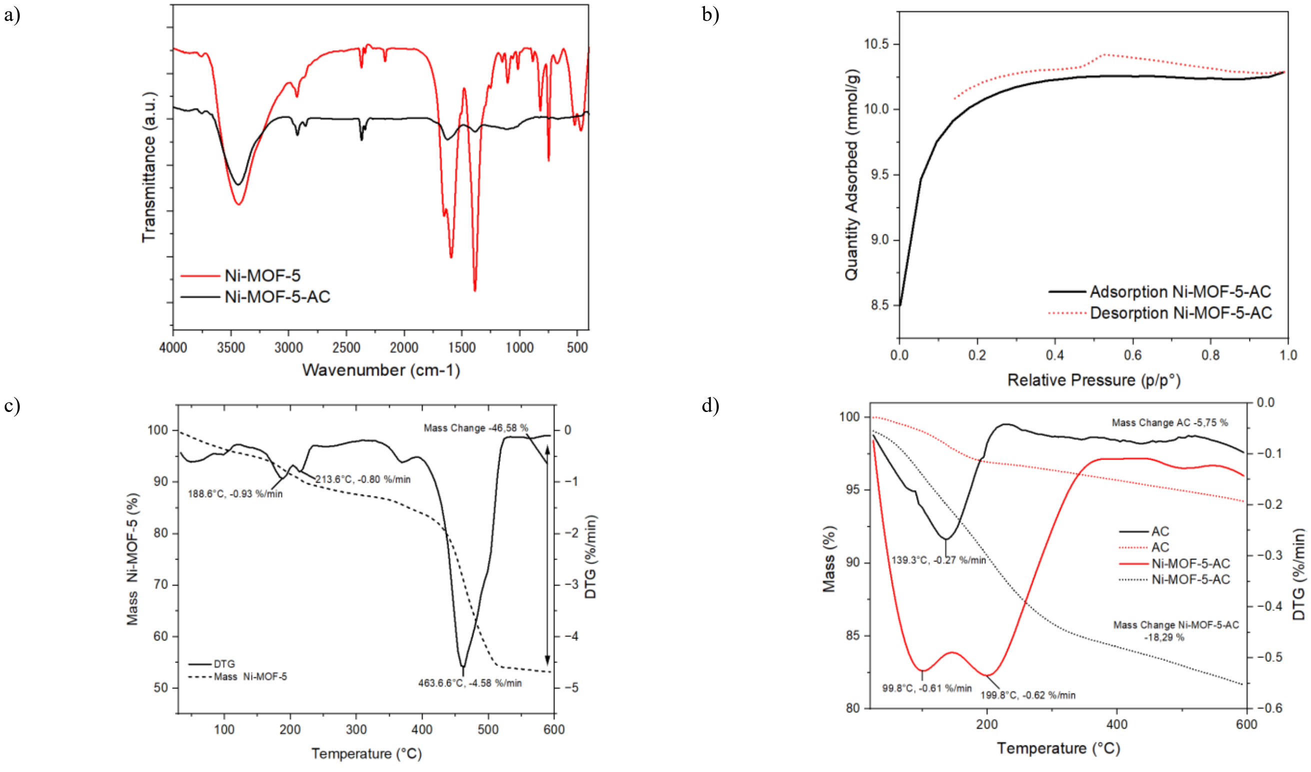

Figure 2. a) Pure Ni-MOF-5 and Ni-MOF-5-AC b) Adsorption-desorption isotherms of N_2 at 77 K for pure Ni-MOF-5 and Ni-MOF-5-AC c) Thermogravimetric analysis (TGA) and differential scanning calorimetry (DSC) for pure Ni-MOF-5 and Ni-MOF-5-AC.

It is important to know the thermal stability of pure MOF, because this material will determine the thermal stability of the hybrid filter material, as it is much less stable than pure activated carbon. Figure 2c shows the results for pure Ni-MOF-5. A progressive loss of mass was observed (dotted line); there is a very slight first inflection in the curve between 180 and 200 °C, mainly due to the evaporation of water (188 °C) and solvent (213°C) absorbed by the solid. Above 200 °C all the water and solvent were evaporated. From 400 °C to 500°C, the greatest mass loss of Ni-MOF-5 was evident, and therefore the decomposition of the porous coordinated polymer structure. The maximum temperature corresponding to the greatest mass loss was 464 °C with a mass loss of 4.58% min^{-1}. The total mass loss of MOF-5 was 46.58%.

Activated carbon, by its nature, is very stable at high temperatures. Figure 2d shows that the total mass loss is 5.75% over 500 °C. The loss of absorbed water was also observed at 139 °C. In the thermogram of the Ni-MOF-5-AC, the evaporation temperatures for both water and adsorbed solvent were observed, in the range between 100 and 200 °C, for both of them. These peaks do not correspond to degradation of the material [26]. The mass loss rate in this range was 0.62% min^{-1}. A slight change is observed between 450 and 500 °C, corresponding to pure Ni-MOF-5. The mass loss of Ni-MOF-5-CA over 500 °C is 18.28%, where 12.54% corresponds to the degradation of the MOFs. Taking into account the total mass loss of pure activated carbon and the hybrid material, it can be inferred that the mass of pure Ni-MOF-5 corresponds to 23.5% of the total mass of the hybrid material.

Adsorption performance

Table 1 shows the summary of adsorption capacity results as a function of concentration of CO_2 in the input stream and the working temperature. It is observed that the adsorption capacity increases with the input CO_2 concentration, which is expected in adsorption processes [27]. For example, when the concentration of CO_2 increases from 5 to 15 and 30% (at 25°C), the CO_2 adsorption capacity was 0.155, 0.398 and 0.828 $mg_{CO2}\ g_{MOF\text{-}AC}^{-1}$, respectively. On the other hand, the effect of the working temperature was observed.

A reduction of the adsorption in the adsorption capacity when the working temperature was increased, in agreeing with other studies. In this case, the adsorption capacity at 50°C was about 78.4% of the adsorption reached at 25°C, while for 100°C, it was about 50.7%. A similar effect is found in the literature regarding the temperature [28]. This occurs given the exothermicity of the adsorption phenomenon and that, as the temperature increases, the energy of the intermolecular forces between the surface of the filter material and the CO_2 molecule decreases, beginning to desorb the CO_2 [29].

Table 1. Adsorption capacity as a function of the CO_2 concentration in the input stream and temperature

Experiment	**CO_2 flux (mL min^{-1})**	**CO_2 concentration** (% vol)	**Adsorption** temperature (°C)	**Adsorption capacity** ($mg_{CO2}\ g_{MOF\text{-}CA}^{-1}$)
1	2.5	5	**25**	0.155
2	7.5	**15**	**25**	0.398
3	15	30	**25**	0.828
4	7.5	**15**	50	0.312
5	7.5	**15**	100	0.202

These results can also be seen in the Figure 3a. Here, the adsorption capacity of CO_2 increases linearly with the concentration of CO_2 in the input stream. The data showed a correlation coefficient of 0.998. The Figure 3b shows the relationship among the adsorption capacity and the working temperature, for a fixed input concentration of CO_2 of 15%. This result suggests that the adsorption corresponds to a physical adsorption type [30]. Figure 3b showed a linear correlation of 0.986. Also, an extrapolation of this curve predicted that the complete desorption of CO_2 would occur at 174 °C. Taking into account this phenomenon, a swing temperature adsorption-desorption process could be combined with a pressure swing adsorption-desorption process (PSA), to reuse the filter for several cycles within a periodic continuous process.

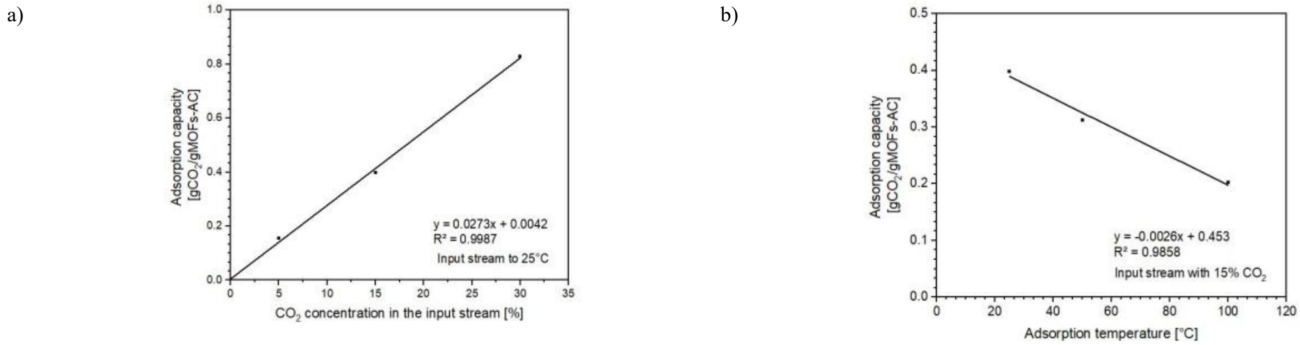

Figure 3. Effect of the input concentration on the final amount of the adsorbed CO_2 by the MOF, b) Effect of the temperature on the adsorbed CO_2 for an-input concentration of 15% CO_2.

Figure 4 shows the adsorption kinetics for the experiments. Here, the volumetric rate of the CO_2 from the output stream was measured. As seen, for the reference material (MgO), the saturation time is reached in shorter times compared to the MOF. These experiments are important to design the adsorption-desorption process.

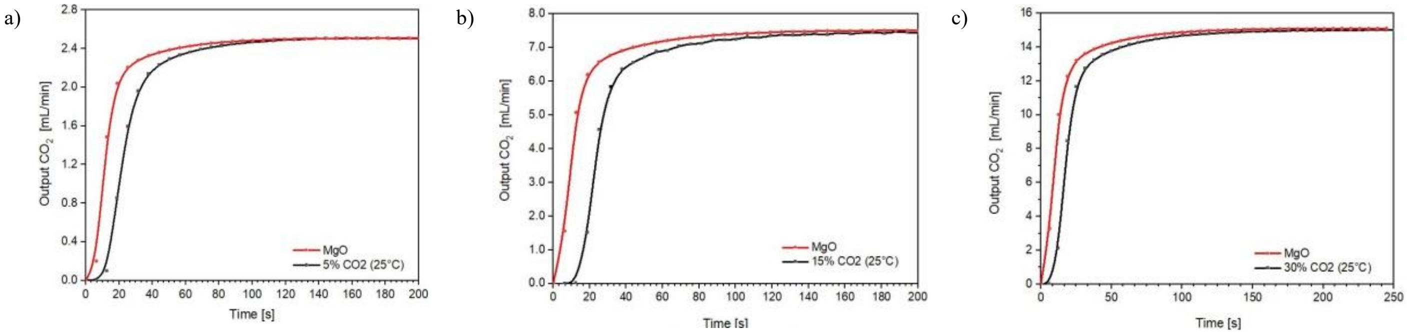

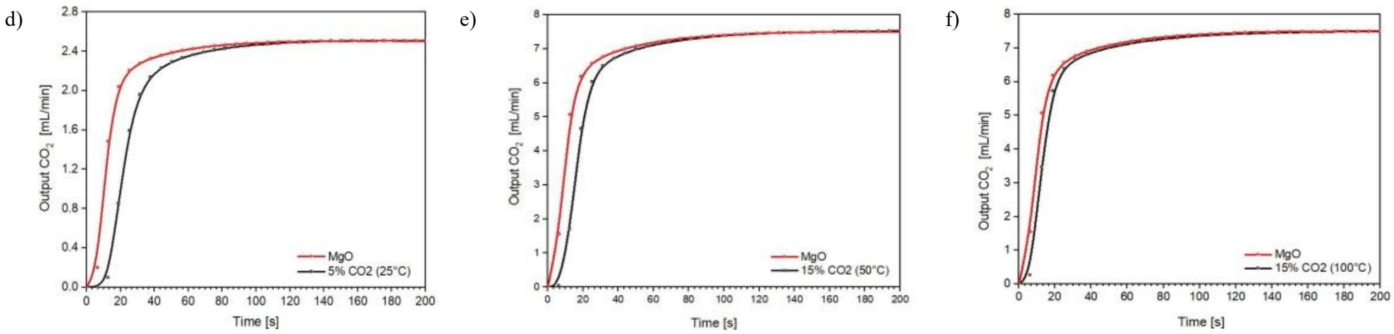

Figure 4. Adsorption dynamics at 25 °C for input of gas with a) 5% CO_2, b) 15% CO_2 and c) 30% CO_2. Adsorption dynamics for and input stream with 15 % CO_2 at d) 25 °C, e) 50 °C and f) 100 ° C.

Finally, the reproducibility of the results is shown in the Table 2. Runs 1 and 2 correspond to the adsorption capacity of the MOFs-AC, while the run 3 correspond to the capacity of the reference material (MgO). At first glance, the MOFs-AC keeps its adsorption capacity for the first essays, showing that the performance is reproducible, for at least some cycles of adsorption. Also, the adsorption capacity compared to MgO is around 35.5 and 37.2%.

Table 2. Adsorption capacity of MOF-AC and reference for an input stream with 5% CO_2 (@ 25°C, 1 atm)

Run name	**CO_2 flux** (**mL** min^{-1})	**CO_2 concentration** (% vol)	**Adsorption T** (°C)	**Adsorption capacity** (mg_{CO2} g^{-1})
1 MOFs-AC	2,5	5	**25**	0.151
2 MOFs-AC	2,5	**5**	**25**	0.158
3 MgO (reference)	2,5	5	**25**	0.425

4. DISCUSION

The production of a pure MOF with the formula NixZn4-x O(BCD)3 (0<x<4) was successfully developed followed by its deposition on the surface of a porous material (activated carbon). The MOF presents a cubic monocrystalline structure when synthesized in pure form. However, in composite form, the crystals were less homogeneous presenting some hexagonal structures on the surface, which has been reported when Nickel has been incorporated into the structure of MOF-5 [16]. The material proved to be thermostable below 200 °C, which is very important for agro-industrial applications. It should be considered that in the case of the hybrid material, the adsorption capacity should be increased for higher working pressures[27]. However, due to equipment problems in the laboratory, pressure tests were not performed. In the studies, MgO was used as a reference material. Although MgO is a known material to adsorb CO_2, its adsorption behavior is different from that of the synthesized material. The adsorption of CO2 on MgO involves the formation of chemical bonds between CO2 molecules and the MgO surface, leading to the production of magnesium carbonate (MgCO3) (chemisorption mechanism), while the adsorption of CO_2 on the synthesized material in this research is a physical adsorption on the surface of the material (physisorption mechanism), based on weak interactions such as van der Waals forces, which is essential for the development of carbon capture technologies [31].

CONCLUSION

The adsorption capacity of the material, although comparable to some studies, is still low for some applications. It could be improved by modifying the surface of the material by adding amino groups to the porous surface of the synthesized material, thus facilitating the formation of intermolecular and intramolecular bonds. These results provide valuable information for optimizing the properties of hybrid materials using MOFs and a solid basis for future research and applications in different scientific areas. However, further progress is still needed in this field to make the material competitive for industrial applications.

FUNDING

This research was funded by Grant Corfo 18CHM-90470 and 18ITE1C-100741. Project IdeA ID23I10274.

REFERENCES

1. J. Zhang, J. Shi, S. Tao, L. Wu, and J. Lu, "Cu2O/Ti3C2MXene heterojunction photocatalysts for improved CO2 photocatalytic reduction performance," Appl. Surf. Sci., vol. 542, no. September 2020, 2021, doi: 10.1016/j.apsusc.2020.148685.
2. W. M. S. Mat Latif, N. M. Sabdullah, S. N. Aenun, and N. A. Bosamah, "A review of global carbon capture and storage (CCS) and carbon capture, utilization, and storage (CCUS)," E3S Web Conf., vol. 516, 2024, [Online]. Available: https://doi.org/10.1051/e3sconf/202451601009
3. H. Bouaboula, J. Chaouki, Y. Belmabkhout, and A. Zaabout, "Comparative review of Direct air capture technologies: From technical, commercial, economic, and environmental aspects," Chem. Eng. J., vol. 484, no. January, p. 149411, 2024, doi: 10.1016/j.cej.2024.149411.
4. K. Zhang and R. Wang, "A critical review on new and efficient adsorbents for CO2 capture," Chem. Eng. J., vol. 485, no. January, p. 149495, 2024, doi: 10.1016/j.cej.2024.149495.
5. Z. Sun, Y. Liao, X. Zhang, and S. XIangzhen, "Research progress in metal–organic frameworks (MOFs) in CO2 capture from post-combustion coal-fired flue gas: characteristics, preparation, modification and applications," J. Mater. Chem. A, no. 10, pp. 5174–5211, 2022.
6. C. Xiao, J. Tian, Q. Chen, and M. Hong, "Water-stable metal-organic frameworks (MOFs): rational construction and carbon dioxide capture," Chem. Sci., vol. 15, no. 5, pp. 1570–1610, 2024, doi: 10.1039/d3sc06076d.
7. H. K. Okoro, S. O. Ayika, J. C. Ngila, and A. C. Tella, "Rising profile on the use of metal–organic frameworks (MOFs) for the removal of heavy metals from the environment: an overview," Appl. Water Sci., vol. 8, no. 6, pp. 1–10, 2018, doi: 10.1007/s13201-018-0818-3.
8. Ji. Liu, P. Thallapally, B. McGrail, D. Brown, and J. Liu, "Progress in adsorption-based CO2 capture by metal–organic frameworks," Chem. Soc. Rev., no. 41, pp. 2308–2322, 2012.
9. H. Yang et al., "Progress in carbon dioxide separation and capture: A review," J. Environ. Sci., vol. 20, no. 1, pp. 14–27, 2008, doi: 10.1016/S1001-0742(08)60002-9.
10. B. Streppel and M. Hirscher, "BET specific surface area and pore structure of MOFs determined by hydrogen adsorption at 20 K," Phys. Chem. Chem. Phys., no. 13, pp. 3220–3222, 2011.
11. O. K. Farha et al., "De novo synthesis of a metal–organic framework material featuring ultrahigh surface area and gas storage capacities," Nat. Chem., vol. 2, no. 11, pp. 944–948, 2010, doi: 10.1038/nchem.834.
12. J. Letwaba, U. O. Uyor, M. L. Mavhungu, N. O. Achuka, and P. A. Popoola, "A review on MOFs synthesis and effect of their structural characteristics for hydrogen adsorption," RSC Adv., vol. 14, no. 20, pp. 14233–14253, 2024, doi: 10.1039/D4RA00865K.
13. H. Li, M. Eddaoudi, M. O'Keeffe, and O. M. Yaghi, "Design and synthesis of an exceptionally stable and highly porous metal-organic framework," Nature, vol. 402, no. 6759, pp. 276–279, 1999, doi: 10.1038/46248.
14. J. A. Greathouse and M. D. Allendorf, "The Interaction of Water with MOF-5 Simulated by Molecular Dynamics," J. Am. Chem. Soc., vol. 128, no. 33, pp. 10678–10679, Aug. 2006, doi: 10.1021/ja063506b.
15. A. Katoch, R. Bhardwaj, N. Goyal, and S. Gautam, "Synthesis, structural and optical study of Ni-doped Metal-organic framework for adsorption based chemical sensor application," Vacuum, vol. 158, pp. 249–256, 2018, doi: https://doi.org/10.1016/j.vacuum.2018.09.019.

16. J.-M. Yang, Q. Liu, and W.-Y. Sun, "Shape and size control and gas adsorption of Ni(II)-doped MOF-5 nano/microcrystals," Microporous Mesoporous Mater., vol. 190, pp. 26–31, 2014, doi: https://doi.org/10.1016/j.micromeso.2014.01.020.
17. H. Li, W. Shi, K. Zhao, H. Li, Y. Bing, and P. Cheng, "Enhanced Hydrostability in Ni-Doped MOF-5," Inorg. Chem., vol. 51, no. 17, pp. 9200–9207, Sep. 2012, doi: 10.1021/ic3002898.
18. X.-W. Liu, T.-J. Sun, J.-L. Hu, and S.-D. Wang, "Composites of metal–organic frameworks and carbon-based materials: preparations, functionalities and applications," J. Mater. Chem. A, vol. 4, no. 10, pp. 3584–3616, 2016, doi: 10.1039/C5TA09924B.
19. Q. L. Zhu and Q. Xu, "Metal-organic framework composites," Chem. Soc. Rev., vol. 43, no. 16, pp. 5468–5512, 2014, doi: 10.1039/c3cs60472a.
20. K. A. Adegoke et al., "Metal-organic framework composites for electrochemical CO2 reduction reaction," Sep. Purif. Technol., vol. 341, p. 126532, 2024, doi: https://doi.org/10.1016/j.seppur.2024.126532.
21. H. N. Nguyen et al., "Investigation on cost-effective composites for CO2 adsorption from post-gasification residue and metal organic framework," J. Environ. Sci., vol. 148, pp. 174–187, 2025, doi: https://doi.org/10.1016/j.jes.2023.10.022.
22. R. Gonzalez-Olmos, A. Gutierrez-Ortega, J. Sempere, and R. Nomen, "Zeolite versus carbon adsorbents in carbon capture: A comparison from an operational and life cycle perspective," J. CO2 Util., vol. 55, p. 101791, 2022, doi: https://doi.org/10.1016/j.jcou.2021.101791.
23. H. Jensen et al., "Determination of size distributions in nanosized powders by TEM, XRD, and SAXS," J. Exp. Nanosci., vol. 1, no. 3, pp. 355–373, Sep. 2006, doi: 10.1080/17458080600752482.
24. M. Malbenia John et al., "An overview on the key advantages and limitations of batch and dynamic modes of biosorption of metal ions," Chemosphere, vol. 357, p. 142051, 2024, doi: https://doi.org/10.1016/j.chemosphere.2024.142051.
25. H. Zhao, H. Song, and L. Chou, "Nickel nanoparticles supported on MOF-5: Synthesis and catalytic hydrogenation properties," Inorg. Chem. Commun., vol. 15, pp. 261–265, 2012, doi: https://doi.org/10.1016/j.inoche.2011.10.040.
26. T. Birsa Čelič et al., "Study of Hydrothermal Stability and Water Sorption Characteristics of 3-Dimensional Zn-Based Trimesate," J. Phys. Chem. C, vol. 117, no. 28, pp. 14608–14617, Jul. 2013, doi: 10.1021/jp4036327.
27. J. Ling, A. Ntiamoah, P. Xiao, P. A. Webley, and Y. Zhai, "Effects of feed gas concentration, temperature and process parameters on vacuum swing adsorption performance for CO2 capture," Chem. Eng. J., vol. 265, pp. 47–57, 2015, doi: https://doi.org/10.1016/j.cej.2014.11.121.
28. H. Ramezanipour Penchah, A. Ghaemi, and F. Jafari, "Piperazine-modified activated carbon as a novel adsorbent for CO2 capture: modeling and characterization," Environ. Sci. Pollut. Res., vol. 29, no. 4, pp. 5134–5143, 2022, doi: 10.1007/s11356-021-16040-5.
29. C. Guan, S. Liu, C. Li, Y. Wang, and Y. Zhao, "The temperature effect on the methane and CO2 adsorption capacities of Illinois coal," Fuel, vol. 211, pp. 241–250, 2018, doi: https://doi.org/10.1016/j.fuel.2017.09.046.
30. P. Puspitasari, S. Sukarni, and A. Hamzah, "Effect of MnFe2O4 Nanoparticles to Reduce CO and HC Levels on Vehicle Exhaust Gas Emissions," J. Mech. Eng. Sci. Technol., vol. 2, no. 1, pp. 27–37, 2018, doi: 10.17977/um016v2i12018p027.
31. G.-B. Elvira, G.-C. Francisco, S.-M. Víctor, and M.-L. R. Alberto, "MgO-based adsorbents for CO2 adsorption: Influence of structural and textural properties on the CO2 adsorption performance," J. Environ. Sci., vol. 57, pp. 418–428, 2017, doi: https://doi.org/10.1016/j.jes.2016.11.016.